

The Large Number Limit of Multifield Inflation

Zhong-Kai Guo^{1,2,*}

¹*CAS Key Laboratory of Theoretical Physics, Institute of Theoretical Physics,
Chinese Academy of Sciences, Beijing 100190, China*

²*School of Physical Sciences, University of Chinese Academy of Sciences, No. 19A Yuquan Road, Beijing 100049, China*
(Dated: December 14, 2024)

We compute the tensor spectral index n_t , tensor-to-scalar ratio r , consistency relation and other inflation parameters in the general monomial multifield slow-roll inflation models with potentials $V \sim \sum_i \lambda_i |\phi_i|^{p_i}$ analytically. The general models give a novel relation that the tensor and scalar spectral index n_t , n_s and also the consistency relation n_t/r are all nearly proportional to the logarithm of the number of fields N_f when N_f is getting extremely large with the order of magnitude around $\mathcal{O}(10^{40})$. Requiring the slow variation parameter $\epsilon \lesssim 0.1$ then gives the upper bound of N_f with $N_f \lesssim N_* e^{ZN_*}$ where N_* is the number of e-foldings before the end of inflation and Z is a value depends on the specific probability distributions of λ_i and p_i . We also find a relation between the inflationary observables which is independent of the specific probability distributions. Besides, n_t/r is differ from the single-field result $-1/8$ with substantial probability except for a few very special cases. In the end, we derive theoretical bounds for tensor-to-scalar ratio $r > 2/N_*$ ($r \gtrsim 0.03$) and for n_t which can be tested by observation in the near future.

I. INTRODUCTION

Inflation [1] has been considered as the standard paradigm for the very early Universe because it naturally solve the flatness, horizon and monopole problems in the hot big bang theory. Furthermore, the quantum fluctuations generated during inflation seed the anisotropies of cosmic microwave background (CMB) and the large-scale structure (LSS) observed in today's Universe [2] which are consistent with experimental observations rather successfully [3–5]. Another significant prediction of inflation models is the primordial gravitational wave. Although astrophysical gravitational waves produced by binary black holes have been detected for sure by LIGO [6], the searching for primordial gravitational wave and its contribution to CMB B-mode polarization is still going on at present and in the future [7–22].

The consistency relation [23] in single-field slow-roll inflation $n_t/r = -1/8$ is a relation between tensor spectral index n_t and the tensor-to-scalar ratio r . It is hoped that the detection of such a compelling signature will supply more validity for inflation theory especially for single-field ones. Sadly the excess of B-mode power detected by BICEP2 [24] can be explained by the polarized thermal dust, not the primordial gravitational wave [25–27].

But otherwise recent experimental progress especially the *Planck* 2015 results [7] shows $r_{0.002} < 0.11$ at 95% C.L. by fitting the *Planck* TT,TE,EE+lowP+lensing combination (P15). The BICEP2 & *Keck Array* B-mode data (BK14) implies $r_{0.05} < 0.09$ (95% C.L.). Combining with *Planck* 2015 TT+lowP+lensing and some other external data, the upper bound on r becomes $r_{0.05} < 0.07$ (95% C.L.) [12, 28] in the base Λ CDM+ r model. The tight constraint on r lead to the chaotic single-field infla-

tion model with a potential $V(\phi) \propto \phi^2$ being disfavored at more than 2σ C.L. [27]. Moreover, single-field inflation models with a monomial potential and the natural inflation model are all marginally disfavored at 95% C.L. and all the single-field inflation models with a convex potential is not favored [28].

On the other hand, many high energy theories contain large numbers of scalar degrees of freedom in extremely high energy scales [29–32], so single-field inflation models are simple but not natural in the very early Universe approaching Planck energy density. In consequence, the study of gravitational wave consistency relation and other inflationary observables for large-number multifield inflation would be necessary and may provide a better representation of our real Universe at the very beginning. Price et al. derived good results for the N_f -monomial models with potential $V \sim \sum_i \lambda_i |\phi_i|^p$ by marginalizing probability random method and many-field limit [33]. But diverse exponent p will be more appropriate and more consistent with many high energy theories [34–41].

In this paper we will derive robust results for n_t/r and other inflationary parameters in N_f -monomial models with diverse exponent p_i . In Sec. II, firstly we present the basics in N_f multifield models, then we use δ N-formalism, central limit theorem (CLT) and Laplace method sequentially to calculate the expectations and corresponding variances of all the inflation parameters and prove their robustness. Some numerical verifications and intuitive graphic representations are showed afterwards for some well-motivated prior probabilities for the λ_i , p_i and initial conditions. We conclude in Sec. III.

*guozhk@itp.ac.cn

II. THE GENERAL LARGE N_f MULTIFIELD MONOMIAL MODELS

We consider the multifield inflation with potential

$$V = \sum_{i=1}^{N_f} V_i(\phi_i) = \sum_{i=1}^{N_f} \lambda_i |\phi_i|^{p_i}, \quad (1)$$

where ϕ_i is the inflaton field, N_f is the number of fields and λ_i , p_i are real, positive constants. For every ϕ_i we have Klein-Gorden equation

$$\ddot{\phi}_i + 3H\dot{\phi}_i + V'_i = 0, \quad (2)$$

where $V'_i \equiv dV_i/d\phi_i$. From Einstein's equation we derive the Friedman equations

$$3H^2 = V + \sum_i \frac{1}{2} \dot{\phi}_i^2, \quad (3)$$

$$\dot{H} = - \sum_i \frac{1}{2} \dot{\phi}_i^2. \quad (4)$$

For simplicity, we set the reduced Planck mass $M_{pl} = 1/\sqrt{8\pi G} \equiv 1$. And the slow-roll inflation arises if the slow-roll parameters are small

$$\epsilon_i \equiv \frac{1}{2} \frac{V_i'^2}{V^2} \ll 1, \quad \eta \equiv \frac{V_i''}{V} \ll 1, \quad \epsilon = \sum_i \epsilon_i \ll 1.$$

Then the second-order derivative term in Eq. (2) could be neglected and the same with the kinetic energy term in contrast to the potential term in Eq. (3)

$$3H\dot{\phi}_i \approx -V'_i, \quad (5)$$

$$3H^2 \approx V = \sum_i V_i. \quad (6)$$

As a consequence of Eq. (5)

$$-\frac{d\phi_i}{V'_i} = \frac{dt}{3H}. \quad (7)$$

To the first-order in slow-roll we have $n_t = -2\epsilon$ where

$$\epsilon = \frac{1}{2} \sum_i \left(\frac{V'_i}{V} \right)^2. \quad (8)$$

In δN -formalism, applying initial flat slice of space-time at time t_* , then the number of e-folds N_* from t_* when the pivot scale k_* leaves the horizon to the end of inflation at t_c [42, 43] is

$$N_* = - \int_{\phi_*}^{\phi_c} \sum_i \frac{V_i}{V'_i} d\phi_i \quad (9)$$

where $\phi_{i,*}$ and $\phi_{i,c}$ denote values at the horizon crossing time and the end of inflation respectively. Substitute V_i and $V'_i = \lambda_i p_i |\phi_i|^{p_i-1}$ then

$$N_* = \frac{1}{2} \sum_i \frac{1}{p_i} (\phi_{i,*}^2 - \phi_{i,c}^2). \quad (10)$$

We can also express the gauge-invariant curvature perturbation ζ by the field perturbations at horizon crossing

$$\zeta \approx \sum_i N_{*,i} \delta\phi_{i,*}, \quad (11)$$

where $N_{*,i} \equiv \partial N_*/\partial\phi_i$. The power spectrum of scalar field perturbations around a smooth background at time t_* is

$$P_{\delta\phi}^{ij} = \left(\frac{H_*}{2\pi} \right)^2 \delta^{ij}. \quad (12)$$

Consequently, the power spectrum of curvature perturbation is

$$P_\zeta = \sum_i N_{*,i} N_{*,i} \left(\frac{H_*}{2\pi} \right)^2. \quad (13)$$

Recalling the tensor power spectrum $P_h = 2H_*^2/\pi^2$ finally comes to the expression of tensor-to-scalar ratio in δN -formalism

$$r = \frac{8}{\sum_i N_{*,i} N_{*,i}}. \quad (14)$$

For N_f -monomial models, it is reasonable to neglect the field values $\phi_{i,c}$ at the end of inflation, i.e., we apply the horizon crossing approximation (HCA). From the definitions of scalar spectral index n_s and ϵ we can derive the n_s

$$n_s - 1 = \frac{d \ln \sum_i N_{*,i} N_{*,i}}{dN} - 2\epsilon, \quad (15)$$

where we have taken the first order approximation of ϵ . Substituting Eq. (5) and Eq. (7) and the relation $dN = Hdt$ into the left term of the right side of the above equation comes to

$$\frac{d \ln \sum_i N_{*,i} N_{*,i}}{dN} = \frac{-2}{\sum_i N_{*,i} N_{*,i}} \frac{1}{V} \sum_i V'_i N_{*,i} N_{*,i}$$

In our general N_f -monomial model the V and N_* are Eq. (1) and Eq. (10) respectively and using HCA then

$$\frac{d \ln \sum_i N_{*,i} N_{*,i}}{dN} = \frac{-2}{\sum_i \phi_i^2/p_i^2} \frac{\sum_j (\lambda_j/p_j) |\phi_j|^{p_j}}{\sum_l \lambda_l |\phi_l|^{p_l}}, \quad (16)$$

where ϕ_i means the field values $\phi_{i,*}$ at horizon crossing. Finally the scalar spectral index n_s in the first order of ϵ is

$$n_s - 1 = - \frac{2}{\sum_i \phi_i^2/p_i^2} \frac{\sum_j (\lambda_j/p_j) |\phi_j|^{p_j}}{\sum_l \lambda_l |\phi_l|^{p_l}} - 2\epsilon. \quad (17)$$

Other inflation parameters in explicit expressions of ϕ_i ,

p_i, λ_i are as follows

$$\epsilon = \frac{1}{2} \frac{\sum_i \lambda_i^2 p_i^2 |\phi_i|^{2p_i-2}}{\left(\sum_j \lambda_j |\phi_j|^{p_j}\right)^2}, \quad (18)$$

$$n_t = -\frac{\sum_i \lambda_i^2 p_i^2 |\phi_i|^{2p_i-2}}{\left(\sum_j \lambda_j |\phi_j|^{p_j}\right)^2}, \quad (19)$$

$$r = \frac{8}{\sum_i \phi_i^2 / p_i^2}, \quad (20)$$

$$\frac{n_t}{r} = -\frac{1}{8} \frac{\sum_i \lambda_i^2 p_i^2 |\phi_i|^{2p_i-2}}{\left(\sum_j \lambda_j |\phi_j|^{p_j}\right)^2} \sum_l \frac{\phi_l^2}{p_l^2}. \quad (21)$$

We set up the probability distribution for the parameters Eq. (17)-(21) by marginalizing them over $P(\lambda)$, $P(\phi_*)$, and $P(p)$ and then calculate their expectations and corresponding variances by applying the central limit theorem (CLT) in the large-number-field limit in the order of magnitude about $N_f > \mathcal{O}(100)$. To further simplify the expressions, we put N_f to really large in the order $\mathcal{O}(10^{40})$ and use Laplace method to produce the final analytical results precisely. The different choice of initial conditions has a very weak effect on the density spectra [44] and applying the HCA in Eq. (10) implies that $P(\phi_*)$ is a uniform prior on the surface of an N_f ellipsoid whose elliptic radii are determined by $P(p)$. So we can sample the ellipsoid by defining

$$\phi_i = \sqrt{\frac{2p_i N_*}{\sum_j x_j^2}} x_i \quad \text{for } \vec{x} \sim \mathcal{N}(0, \mathbb{1}), \quad (22)$$

where $\mathcal{N}(0, \mathbb{1})$ is the multivariate normal distribution. Then one of the summations in Eq. (17)-(21) is

$$\sum_i \lambda_i^2 p_i^2 |\phi_i|^{2p_i-2} = \sum_i \frac{\lambda_i^2 2^{p_i-1} p_i^{p_i+1} N_*^{p_i-1} |x_i|^{2p_i-2}}{\sqrt{\sum_j x_j^2}^{(2p_i-2)}}. \quad (23)$$

In many-field limit $N_f \rightarrow \infty$ the CLT ensures that the summation is normally distributed with mean

$$\left\langle \sum_i \lambda_i^2 p_i^2 |\phi_i|^{2p_i-2} \right\rangle_{N_f \uparrow} = N_f \langle \lambda^2 \rangle \left\langle \frac{2^{p-1} p^{p+1} N_*^{p-1} |x|^{2p-2}}{\sqrt{N_f}^{(2p-2)}} \right\rangle \quad \left\langle \sum_i \phi_{i,*}^2 / p_i^2 \right\rangle_{N_f \uparrow} = 2N_* \left\langle \frac{1}{p} \right\rangle. \quad (24)$$

in which we assume that the λ_i, p_i and x_i are independent and angle brackets $\langle \cdot \rangle$ indicates the expectation value. The lower term of denominator in Eq. (23) $\sqrt{\sum_j x_j^2}$ is χ -distribution and approaches normal distribution $\mathcal{N}(\sqrt{N_f}, 1/\sqrt{2})$ in many-field limit. Besides, for any normally distributed variable $x \sim \mathcal{N}(\mu, \sigma)$ [45]

$$\langle |x|^\nu \rangle = \frac{2^{(\nu/2)} \sigma^\nu}{\sqrt{\pi}} \Gamma\left(\frac{1+\nu}{2}\right) F_{1,1}\left(-\frac{\nu}{2}; \frac{1}{2}; -\frac{\mu^2}{2\sigma^2}\right), \quad (25)$$

where $F_{1,1}$ is the confluent hypergeometric function of the first kind and $\nu > -1$. And if $\nu < -1$, $\langle |x|^\nu \rangle$ may diverge. As for $\mu = 0, \sigma = 1$, then $F_{1,1} = 1$, the result becomes

$$\langle |x|^\nu \rangle = \frac{2^{(\nu/2)}}{\sqrt{\pi}} \Gamma\left(\frac{1+\nu}{2}\right). \quad (26)$$

Also we know the ratio distribution α/β for normally distributed random variables (RVs) $\alpha \sim \mathcal{N}(\mu_\alpha, \sigma_\alpha)$ and $\beta \sim \mathcal{N}(\mu_\beta, \sigma_\beta)$ as $P(\beta > 0) \rightarrow 1$ will approach a normal distribution with mean μ_α/μ_β and standard deviation [46]

$$s = \frac{\sqrt{\mu_\beta^2 \sigma_\alpha^2 - 2\gamma \mu_\alpha \mu_\beta \sigma_\alpha \sigma_\beta + \mu_\alpha^2 \sigma_\beta^2}}{\mu_\beta^2} \quad (27)$$

in large N_f limit, where $\gamma \equiv \langle (\alpha - \mu_\alpha)(\beta - \mu_\beta) \rangle / (\sigma_\alpha \sigma_\beta) \in [-1, 1]$ is the correlation. The term $(\sum_i \lambda_i |\phi_{i,*}|^p)^2$ is also approximately normal in the large N_f limit and we can prove the relation

$$\left\langle \left(\sum_i \lambda_i |\phi_i|^{p_i} \right)^2 \right\rangle = \left\langle \sum_i \lambda_i |\phi_i|^{p_i} \right\rangle^2 \quad \text{as } N_f \rightarrow \infty. \quad (28)$$

Then in the large N_f limit the mean of the summation

$$\left\langle \sum_i \lambda_i^2 p_i^2 |\phi_i|^{2p_i-2} \right\rangle = \frac{N_f}{\sqrt{\pi}} \langle \lambda^2 \rangle \left\langle \frac{N_*^{p-1}}{N_f^{p-1}} 2^{2p-2} p^{p+1} \Gamma(p - \frac{1}{2}) \right\rangle \quad (29)$$

is finite when $p > 1/2$. Similarly, the means of other summations are

$$\left\langle \sum_i \lambda_i |\phi_i|^{p_i} \right\rangle_{N_f \uparrow} = \frac{N_f}{\sqrt{\pi}} \langle \lambda \rangle \left\langle \left(\frac{N_*}{N_f} \right)^{\frac{p}{2}} 2^p p^{\frac{p}{2}} \Gamma\left(\frac{p}{2} + \frac{1}{2}\right) \right\rangle, \quad (30)$$

$$\left\langle \sum_j \frac{\lambda_j}{p_j} |\phi_j|^{p_j} \right\rangle_{N_f \uparrow} = \frac{N_f}{\sqrt{\pi}} \langle \lambda \rangle \left\langle \left(\frac{N_*}{N_f} \right)^{\frac{p}{2}} 2^p p^{(\frac{p}{2}-1)} \Gamma\left(\frac{p}{2} + \frac{1}{2}\right) \right\rangle, \quad (31)$$

$$\left\langle \sum_i \phi_{i,*}^2 / p_i^2 \right\rangle_{N_f \uparrow} = 2N_* \left\langle \frac{1}{p} \right\rangle. \quad (32)$$

And the standard deviations can be calculated from the mean values and the corresponding two-moments so they are tedious algebraic functions of $\langle \lambda \rangle, \langle \lambda^2 \rangle, \langle \lambda^4 \rangle$ and many other terms. But particularly, the standard deviations of Eq. (32) is relative compact

$$s = \frac{2N_*}{\sqrt{N_f}} \sqrt{3\mu_{1/p^2} - 2\sqrt{2}\gamma' \mu_{1/p} \sqrt{3\mu_{1/p^2} - \mu_{1/p}^2}} \\ \propto \frac{1}{\sqrt{N_f}} \rightarrow 0 \quad \text{as } N_f \rightarrow \infty, \quad (33)$$

where γ' is the correlation between the numerator and denominator in Eq. (32). Finally by applying the Eq.

(27) and other conclusions in many-field limit the value of r is normally distributed with a mean

$$\langle r \rangle = \frac{4}{N_* \langle 1/p \rangle}, \quad (34)$$

and a standard deviation proportional to

$$s_r = \frac{1}{\sqrt{N_f}} \frac{4}{N_*} \frac{\sqrt{3\sigma_{1/p}^2 + 4\mu_{1/p}^2 - 2\sqrt{2}\gamma''\mu_{1/p}\sqrt{3\sigma_{1/p}^2 + 2\mu_{1/p}^2}}}{\mu_{1/p}^2} \\ \propto \frac{1}{\sqrt{N_f}} \rightarrow 0 \quad \text{as } N_f \rightarrow \infty. \quad (35)$$

The value of n_t is normally distributed with a mean

$$\langle n_t \rangle = -2\langle \epsilon \rangle = -\frac{\sqrt{\pi} \langle \lambda^2 \rangle}{4N_* \langle \lambda \rangle^2} \frac{\langle 2^{2p}(N_*/N_f)^p p^{p+1} \Gamma(p - \frac{1}{2}) \rangle}{\langle 2^p(N_*/N_f)^{p/2} p^{p/2} \Gamma(\frac{p}{2} + \frac{1}{2}) \rangle^2} \\ \approx -\frac{\sqrt{\pi} \langle \lambda^2 \rangle}{4N_* \langle \lambda \rangle^2} \frac{p_m \Gamma(p_m - \frac{1}{2})}{4\Gamma^2(\frac{p_m+1}{2})} \frac{1}{f(p_m)} \ln\left(\frac{N_f}{N_*}\right), \quad (36)$$

where p_m is the minimum possible value and $f(p)$ is the probability density function of p . Note that a finite prediction for mean requires $p > 1/2$ and a finite standard deviation requires $p > 3/4$. To get the approximation Eq. (37) we have used Laplace method (see Appendix A). And both the standard deviations of n_t and ϵ are proportional to

$$s_{n_t} = 4s_\epsilon \propto \frac{1}{\sqrt{N_f}} \rightarrow 0 \quad \text{as } N_f \rightarrow \infty. \quad (38)$$

The value of consistency relation n_t/r is a multiplication of two normally distributed asymptotic-sharp random variate with a mean

$$\left\langle \frac{n_t}{r} \right\rangle_{N_f \uparrow} = -\frac{1}{8} \frac{\langle \lambda^2 \rangle}{\langle \lambda \rangle^2} \left\langle \frac{1}{p} \right\rangle \frac{\sqrt{\pi} \langle 2^{2p}(N_*/N_f)^p p^{p+1} \Gamma(p - \frac{1}{2}) \rangle}{2 \langle 2^p(N_*/N_f)^{p/2} p^{p/2} \Gamma(\frac{p}{2} + \frac{1}{2}) \rangle^2} \\ \approx -\frac{1}{8} \frac{\langle \lambda^2 \rangle}{\langle \lambda \rangle^2} \left\langle \frac{1}{p} \right\rangle \frac{\sqrt{\pi} p_m \Gamma(p_m - \frac{1}{2})}{8\Gamma^2(\frac{p_m+1}{2})} \frac{1}{f(p_m)} \ln\left(\frac{N_f}{N_*}\right), \quad (39)$$

where the requirements for p is same as above and please see Eq. (B1) in Appendix B for the validity of multiplication splitting. To be more exact, for typical $P(\lambda)$ and $P(p)$, the Eq. (39) will be a very good approximation when N_f is larger than $\mathcal{O}(100)$ but the approximation Eq. (40) is as good as Eq. (39) only in the case N_f is larger than $\mathcal{O}(e^{100}) \sim \mathcal{O}(10^{40})$. And the standard deviation is proportional to

$$s_{n_t/r} \propto \frac{1}{\sqrt{N_f}} \rightarrow 0 \quad \text{as } N_f \rightarrow \infty, \quad (41)$$

and also see Appendix B for the detailed proof.

The value n_s is a combination of two normally distributed variate with a mean

$$\langle n_s \rangle - 1 = -\frac{1}{N_* \langle 1/p \rangle} \frac{\langle (N_*/N_f)^{p/2} 2^p p^{p/2-1} \Gamma(\frac{p}{2} + \frac{1}{2}) \rangle}{\langle (N_*/N_f)^{p/2} 2^p p^{p/2} \Gamma(\frac{p}{2} + \frac{1}{2}) \rangle} - 2\langle \epsilon \rangle \\ \approx -\frac{1}{N_* \langle 1/p \rangle p_m} - \frac{\sqrt{\pi} \langle \lambda^2 \rangle}{4N_* \langle \lambda \rangle^2} \frac{p_m \Gamma(p_m - \frac{1}{2})}{4\Gamma^2(\frac{p_m+1}{2})} \frac{1}{f(p_m)} \ln\left(\frac{N_f}{N_*}\right). \quad (42)$$

and the standard deviation of the left term of the result is also proportional to

$$s_L \propto \frac{1}{\sqrt{N_f}} \rightarrow 0 \quad \text{as } N_f \rightarrow \infty. \quad (43)$$

Requiring the slow variation parameter $\epsilon \lesssim 0.1$ then from Eq. (37) we find the upper limit of N_f is

$$N_f \lesssim N_* \exp(ZN_*) \quad (44)$$

where Z is a value depends on the specific probability distribution of λ_i and p_i

$$Z = \frac{8}{\sqrt{\pi}} \frac{\langle \lambda^2 \rangle}{\langle \lambda \rangle^2} \frac{4\Gamma^2(\frac{p_m+1}{2})}{p_m \Gamma(p_m - \frac{1}{2})} f(p_m) \times \mathcal{O}(10^{-1}). \quad (45)$$

In addition, combining Eq. (34), Eq. (37), Eq. (40) and Eq. (43) immediately reaches the lower limiting value of consistency relation n_t/r

$$\left\langle \frac{n_t}{r} \right\rangle \gtrsim -\frac{N_*}{2} \left\langle \frac{1}{p} \right\rangle \times \mathcal{O}(10^{-1}), \quad (46)$$

and a relation

$$\langle n_s \rangle = 1 - \frac{\langle r \rangle}{4p_m} + \langle n_t \rangle \quad (47)$$

which is independent of specific probability distribution of λ_i , p_i and $\phi_{i,*}$. Adding the restriction $p_m > 1/2$ gives two bounds of r

$$r > \frac{2}{N_*}, \quad (48)$$

$$r > 2(1 - n_s + n_t), \quad (49)$$

and the value range of n_t as

$$\frac{1}{2} \frac{1}{p_m N_*} + n_s - 1 < n_t < 0 \quad (50)$$

which can be tested by observation in the near future because the Eq. (49) means $r \gtrsim 0.03$ which is exactly on the coverage of next generation projects under construction.

Obviously, with all p_i equal we can regain all the conclusions described in [33] and many other classic results from Eq. (39), Eq. (34), Eq. (36), and Eq. (42) while the extent of deviation from the single-field model result

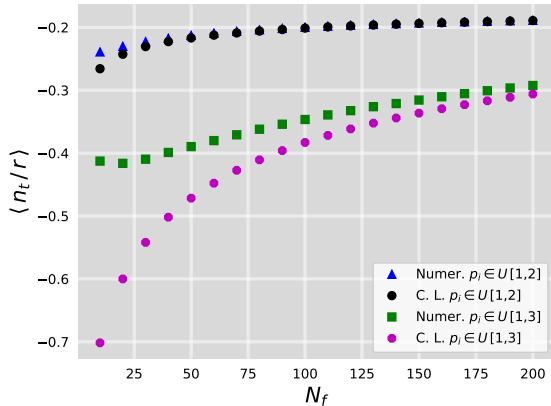


FIG. 1: The multifield prediction from CLT in Eq. (39) compared to the numerical simulations with 100 000 samples, $\lambda_i \in \mathcal{U}[10^{-14}, 10^{-13}]$, $p_i \in \mathcal{U}[1, 2]$ (upper) and $p_i \in \mathcal{U}[1, 3]$ (lower). Using the horizon-crossing approximation, the field values $\phi_{i,*}$ as the pivot scale k_* leaves the horizon are originated from a uniform prior on the surface in Eq. (10).

of $n_t/r = -1/8$ has gotten much larger than the fixed- p ones.

Figure 1 compares the predicted value from CLT in Eq. (39) to corresponding numerical results from Eq. (21) with uniform-distribution $\lambda_i \in \mathcal{U}[10^{-14}, 10^{-13}]$ and uniform-distribution $p_i \in \mathcal{U}[1, 2]$ and $p_i \in \mathcal{U}[1, 3]$ respectively, showing excellent convergence in many-field limit. Moreover, the wider of the distribution of p_i is, the larger N_f is needed for the convergence to be same good. And also we can strictly prove that the corresponding relative error is proportional to $1/N_f$.

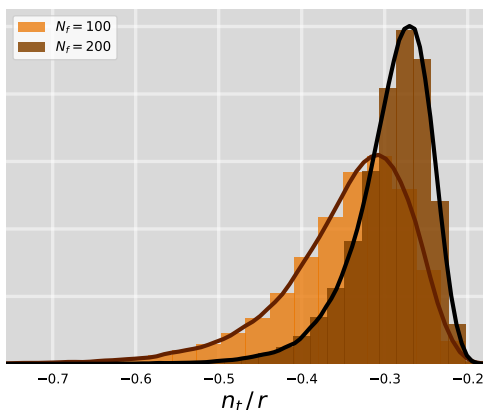


FIG. 2: The probability distributions for n_t/r with histograms built from 100 000 numerical samples with $\lambda_i \in \mathcal{U}[10^{-14}, 10^{-13}]$ and $p_i \in \mathcal{U}[1, 3]$ when N_f is 100 (left) and 200 (right).

Figure 2 delineates the probability distributions functions (PDF) for n_t/r with $\lambda_i \in \mathcal{U}[10^{-14}, 10^{-13}]$ and

$p_i \in \mathcal{U}[1, 3]$ when N_f is 100 and 200 respectively. As shown, the larger that the N_f becomes, the more sharp that the PDF of n_t/r will be and the more likely that the mean of n_t/r can be a good representation of the real value, as proved in Eq. 41.

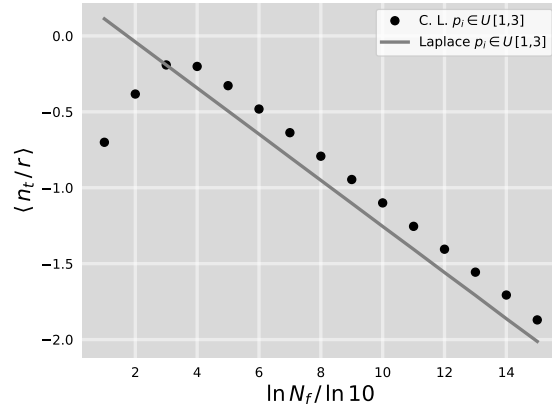


FIG. 3: The multifield analytic prediction from Laplace approximation method in Eq. (40) compared to the central limit results with 1 000 000 samples, $\lambda_i \in \mathcal{U}[10^{-14}, 10^{-13}]$ and $p_i \in \mathcal{U}[1, 3]$. The logarithmic correlation relation is evident in extremely large N_f .

To understand the Laplace approximation result in Eq. (40) more intuitively, we compare the central limit results for $\langle n_t/r \rangle$ in Eq. (39) to the predicted analytical values from Eq. (40) when N_f is extremely large in Figure 3. It is clearly observed that when N_f is small, the Laplace approximation is at a great deviation while the extremely large N_f leads to a good agreement with Eq. (39) and the logarithmic correlation relation is evident. Also the wider distribution of p_i needs the larger N_f for the approximation to be good enough. But in a narrow distribution width of p_i as the setup in the figure, it does not need the N_f to be as large as $\mathcal{O}(10^{40})$ to make the Laplace approximation valid, only $N_f \gtrsim \mathcal{O}(10^5)$. The $N_f \sim \mathcal{O}(10^{40})$ condition is suitable for general cases. Notice that the C. L. results, in such a large N_f , can represent the numerical ones perfectly well according to the aforementioned analysis.

III. CONCLUSIONS

We have computed the probability distributions for the tensor spectral index n_t , tensor-to-scalar ratio r , scalar spectral index n_s , and the consistency relation n_t/r in the general large number monomial multifield inflation model, as a function of the probability distribution of couplings λ_i , power indexes p_i , initial field values and the number of fields N_f . And in the many-field limit, the distributions are all become sharp with the variances $s^2 \propto 1/N_f$, so the expected values we get are very robust.

We give a novel prediction that the inflationary parameters n_t , n_s and n_t/r are all nearly proportional to $\ln N_f$ when N_f is extremely large

$$n_t, n_s, \epsilon, \frac{n_t}{r} \propto \ln N_f \quad \text{as } N_f \rightarrow \infty. \quad (52)$$

And the dependency between ϵ and $\ln N_f$ immediately gives the upper bound of $N_f \lesssim N_* e^{ZN_*}$ if we require ϵ is small enough such as $\mathcal{O}(10^{-1})$ where Z is a value decided by the specific probability distributions of λ_i and p_i . But the tensor-to-scalar ratio r depends only on the probability distribution of p_i

$$r = \frac{4}{N_* \langle 1/p \rangle}, \quad (53)$$

Besides, we find some distribution-independent relations between the inflationary observables and thereby we give some theoretical bounds for r and n_t especially $r > 2/N_*$ ($r \gtrsim 0.03$) which can be tested by observation in the near future. All the predictions above together can distinguish between diverse- p - N_f -monomial models, fixed- p - N_f -monomial models and their single-field analogues. Additionally, exploring a broader class of large number multifield models such as the multifield extension to small-field inflation will be interesting follow-up work. Having found some interesting and testable conclusions of large number multifield inflation in this work, we hope that the large number inflation could be studied more comprehensively in the future for the deep understanding of the very early universe and the physics in extremely high-energy.

Acknowledgments

The author would like to sincerely thank Qing-Guo Huang for careful review, comments, and feedback on this paper. I am also grateful to Shi Pi and Cheng Cheng for helpful discussions. This work is supported by the project 11647601 of National Natural Science Foundation of China. I acknowledge the contribution of HPC Cluster of ITP-CAS.

Appendix A: Laplace method

We define the notations

$$M \equiv \frac{N_f}{N_*} \rightarrow \infty,$$

$$g_1(p) \equiv 2^{2p} p^{p+1} \Gamma(p - \frac{1}{2}) f(p), \quad g_2(p) \equiv 2^p p^{p/2} \Gamma(\frac{p}{2} + \frac{1}{2}) f(p),$$

where $f(p)$ is the possibility density function of p and we restrict $p > 1/2$. Thus we can rewrite one of the upper average terms in Eq. (36) and Eq. (39) by

$$\left\langle 2^{2p} (N_*/N_f)^p p^{p+1} \Gamma(p - \frac{1}{2}) \right\rangle = \int_{p_m}^{p_{max}} e^{-p \ln M} g_1(p) dp, \quad (A1)$$

where p_m and p_{max} are the minimum and the maximum possible value for typical possibility distribution of p , respectively. Then when $M \rightarrow \infty$ we use Laplace method to simplify the expression

$$\begin{aligned} \int_{p_m}^{p_{max}} e^{-p \ln M} g_1(p) dp &\approx g_1(p_m) \int_{p_m}^{p_{max}} e^{-p \ln M} dp \quad (A2) \\ &\approx g_1(p_m) e^{-p_m \ln M} / \ln M, \quad (A3) \end{aligned}$$

where we have dropped the p_{max} term because it decreases much faster than the p_m term when $M \rightarrow \infty$ and the other average term is

$$\left\langle 2^p (N_*/N_f)^{\frac{p}{2}} p^{p/2} \Gamma(\frac{p}{2} + \frac{1}{2}) \right\rangle \approx 2g_2(p_{min}) e^{-\frac{p_{min}}{2} \ln M} / \ln M,$$

Finally the p -average terms in Eq. (36) and Eq. (39) can be expressed in many-field limit by

$$\begin{aligned} \frac{\langle 2^{2p} (N_*/N_f)^p p^{p+1} \Gamma(p - \frac{1}{2}) \rangle}{\langle 2^p (N_*/N_f)^{\frac{p}{2}} p^{p/2} \Gamma(\frac{p}{2} + \frac{1}{2}) \rangle^2} \Big|_{N_f \rightarrow \infty} &\approx \frac{g_1(p_{min})}{4g_2(p_{min})^2} \ln M \\ &= \frac{p_{min} \Gamma(p_{min} - \frac{1}{2})}{4\Gamma^2(\frac{p_{min}+1}{2})} \frac{1}{f(p_{min})} \ln \left(\frac{N_f}{N_*} \right). \end{aligned}$$

Similarly, the p -average term in Eq. (42) is

$$\frac{\langle (N_*/N_f)^{p/2} 2^p p^{(p/2-1)} \Gamma(\frac{p}{2} + \frac{1}{2}) \rangle}{\langle (N_*/N_f)^{p/2} 2^p p^{p/2} \Gamma(\frac{p}{2} + \frac{1}{2}) \rangle} \Big|_{N_f \rightarrow \infty} \approx \frac{1}{p_{min}}.$$

Appendix B: Standard deviation s in the large N_f limit

Generally we suppose there are two normally distributed RVs $X_1 \sim \mathcal{N}(\mu_1, \sigma_1)$, $X_2 \sim \mathcal{N}(\mu_2, \sigma_2)$ and both standard deviations are inversely proportional to the square root of N_f

$$\sigma_1 \propto \frac{1}{\sqrt{N_f}}, \quad \sigma_2 \propto \frac{1}{\sqrt{N_f}},$$

and the correlation coefficient of X_1 and X_2 is

$$\gamma_{x_1 x_2} = \frac{\text{Cov}(X_1, X_2)}{\sigma_1 \sigma_2} = \frac{\langle X_1 X_2 \rangle - \mu_1 \mu_2}{\sigma_1 \sigma_2},$$

and $\gamma_{x_1 x_2}$ satisfy

$$|\gamma_{x_1 x_2}| < 1.$$

as a consequence of Cauchy-Bunyakovsky-Schwarz inequality. Immediately,

$$\langle X_1 X_2 \rangle = \mu_1 \mu_2 + \gamma_{x_1 x_2} \sigma_1 \sigma_2 \rightarrow \mu_1 \mu_2 \quad \text{as } N_f \rightarrow \infty. \quad (B1)$$

Besides, the correlation coefficient of X_1^2 and X_2^2 is

$$\gamma_{x_1^2 x_2^2} = \frac{\text{Cov}(X_1^2, X_2^2)}{\sigma_{X_1^2} \sigma_{X_2^2}} = \frac{\langle X_1^2 X_2^2 \rangle - \langle X_1^2 \rangle \langle X_2^2 \rangle}{\sigma_{X_1^2} \sigma_{X_2^2}},$$

from which we can get

$$\langle X_1^2 X_2^2 \rangle = \sigma_{X_1^2} \sigma_{X_2^2} \gamma_{x_1^2 x_2^2} + (\sigma_1^2 + \mu_1^2)(\sigma_2^2 + \mu_2^2). \quad (\text{B2})$$

Also $\gamma_{x_1^2 x_2^2}$ satisfy

$$|\gamma_{x_1^2 x_2^2}| < 1.$$

From Eq. (25) we note that for any normally distributed variable $X \sim \mathcal{N}(\mu, \sigma)$

$$\langle X^4 \rangle = 3\sigma^4 + 6\mu^2\sigma^2 + \mu^4.$$

where $F_{1,1}$ is the confluent hypergeometric function of the first kind and $F_{1,1}(-2; \frac{1}{2}; z) = 1 - 4z + \frac{4}{3}z^2$. Hence

$$\sigma_{X_1^2}^2 = \langle X_1^4 \rangle - \langle X_1^2 \rangle^2 = 2\sigma_1^4 + 4\mu_1^2\sigma_1^2, \quad (\text{B3})$$

$$\sigma_{X_2^2}^2 = 2\sigma_2^4 + 4\mu_2^2\sigma_2^2. \quad (\text{B4})$$

Then substitute Eq. (B3) and Eq. (B4) into Eq. (B2) we get the standard deviation of the multiplication $X_1 X_2$

$$\begin{aligned} D(X_1 X_2) &= \langle X_1^2 X_2^2 \rangle - \langle X_1 X_2 \rangle^2 \\ &= \gamma_{x_1^2 x_2^2} (4\sigma_1^4 \sigma_2^4 + 8\mu_1^2 \sigma_1^2 \sigma_2^4 + 8\mu_2^2 \sigma_1^4 \sigma_2^2 + 4\mu_1^2 \mu_2^2 \sigma_1^2 \sigma_2^2)^{1/2} \\ &\quad + (1 - \gamma_{x_1 x_2}^2) \sigma_1^2 \sigma_2^2 + \mu_1^2 \sigma_2^2 + \mu_2^2 \sigma_1^2 - 2\gamma_{x_1 x_2} \mu_1 \mu_2 \sigma_1 \sigma_2 \\ &\propto \frac{1}{N_f} \quad \text{as } N_f \rightarrow \infty, \end{aligned}$$

if both μ_1 and μ_2 are not go up faster than N_f^q where q is an arbitrary positive number.

For the left term of Eq. (17)

$$\frac{1}{\sum_i \phi_{i,*}^2 / p_i^2} \frac{\sum_j (\lambda_j / p_j) |\phi_j|^{p_j}}{\sum_l \lambda_l |\phi_l|^{p_l}} \quad (\text{B5})$$

in which

$$X_1 = \frac{1}{\sum_i \phi_{i,*}^2 / p_i^2}, \quad X_2 = \frac{\sum_j (\lambda_j / p_j) |\phi_j|^{p_j}}{\sum_l \lambda_l |\phi_l|^{p_l}},$$

in many-field limit. Then

$$\mu_1 \rightarrow \frac{1}{2N_* \langle 1/p \rangle}, \quad \mu_2 \rightarrow \frac{1}{p_{min}}$$

are all independent of N_f which means the standard deviation

$$s_L \propto \frac{1}{\sqrt{N_f}}.$$

Else for the term in consistency relation Eq. (21)

$$\frac{\sum_i \lambda_i^2 p_i^2 |\phi_i|^{2p_i-2}}{(\sum_j \lambda_j |\phi_j|^{p_j})^2} \sum_l \frac{\phi_{l,*}^2}{p_l^2} \quad (\text{B6})$$

in which

$$X_1 = \frac{\sum_i \lambda_i^2 p_i^2 |\phi_i|^{2p_i-2}}{(\sum_j \lambda_j |\phi_j|^{p_j})^2}, \quad X_2 = \sum_l \frac{\phi_{l,*}^2}{p_l^2},$$

in the many-field limit. And their means satisfy the condition

$$\mu_1 \propto \ln N_f < N_f^q, \quad \mu_2 \rightarrow \text{Const.} \propto N_f^0 < N_f^q.$$

Obviously we have proved the asymptotic inverse square root relation of the standard deviation of n_t/r

$$s_{n_t/r} \propto \frac{1}{\sqrt{N_f}}, \quad \text{as } N_f \rightarrow \infty.$$

-
- [1] A. A. Starobinsky, Phys. Lett. B **91**, 99 (1980); A. H. Guth, Phys. Rev. D **23**, 347 (1981); A. D. Linde, Phys. Lett. B **108**, 389 (1982); A. Albrecht and P. J. Steinhardt, Phys. Rev. Lett. **48**, 1220 (1982).
- [2] V. F. Mukhanov, H. A. Feldman and R. H. Brandenberger, Phys. Rept. **215**, 203 (1992).
- [3] E. Komatsu *et al.*, Seven-year Wilkinson Microwave Anisotropy Probe (WMAP) Observations: Cosmological Interpretation, ApJS **192**, 18 (2011).
- [4] Planck Collaboration *et al.*, Planck 2013 results. XXII. Constraints on inflation, Astronomy & Astrophysics **571**, A22 (2014).
- [5] P. Collaboration *et al.*, Planck 2015. XX. Constraints on inflation, arXiv:1502.02114.
- [6] B. P. Abbott *et al.* [LIGO Scientific and Virgo Collaborations], Phys. Rev. Lett. **116**, no. 6, 061102 (2016) arXiv:1602.03837.
- [7] P. A. R. Ade *et al.* [Planck Collaboration], arXiv:1502.01589.
- [8] M. Remazeilles *et al.* [CORE Collaboration], arXiv:1704.04501.
- [9] T. Matsumura *et al.*, J. Low. Temp. Phys. **184**, no. 3-4, 824 (2016).
- [10] D. Baumann *et al.* [CMBPol Study Team], AIP Conf. Proc. **1141**, 10 (2009) arXiv:0811.3919.
- [11] P. Andre *et al.* [PRISM Collaboration], arXiv:1306.2259.
- [12] P. A. R. Ade *et al.* [BICEP2 and Keck Array Collaborations], Phys. Rev. Lett. **116**, 031302 (2016) arXiv:1510.09217.
- [13] Zhang X M, Jing Y P. Editorial. Sci China-Phys Mech Astron, 2014, 57: 1413; Li H, Li M Z, Qiu T T *et al.* Sci China-Phys Mech Astron, 2014, 57: 1431-1441; Cheng C, Huang Q G, Zhao W, Sci China-Phys Mech Astron, 2014, 57: 1460-1465.
- [14] J. A. Grayson *et al.*, [BICEP3 Collaboration], Proc. SPIE Int. Soc. Opt. Eng. **9914**, 99140S (2016) arXiv:1607.04668.
- [15] S. W. Henderson *et al.*, J. Low. Temp. Phys. **184**, no. 3-4, 772 (2016) arXiv:1510.02809.
- [16] K. Harrington *et al.*, Proc. SPIE Int. Soc. Opt. Eng. **9914**, 99141K (2016) arXiv:1608.08234.
- [17] B. A. Benson *et al.*, [SPT-3G Collaboration], Proc. SPIE Int. Soc. Opt. Eng. **9153**, 91531P (2014) arXiv:1407.2973.
- [18] K. Arnold *et al.*, Proc. SPIE, Millimeter, Submillimeter, and Far-Infrared Detectors and Instrumentation for Astronomy VII, **9153**, 91531F (2014).
- [19] A. M. Aboobaker *et al.*, [EBEX Experiment], arXiv:1703.03847.
- [20] J. M. Nagy *et al.*, [SPIDER Collaboration], Astrophys. J. **844**, no. 2, 151 (2017) arXiv:1704.00215.
- [21] K. W. Masui and U. L. Pen, Phys. Rev. Lett. **105**, 161302 (2010) arXiv:1006.4181.
- [22] L. Book, M. Kamionkowski and F. Schmidt, Phys. Rev. Lett. **108**, 211301 (2012) arXiv:1112.0567.
- [23] E. J. Copeland, E. W. Kolb, A. R. Liddle, and J. E. Lidsey, Phys. Rev. Lett. **71**, 219 (1993).
- [24] P. A. R. Ade *et al.*, [BICEP2 Collaboration], Phys. Rev. Lett. **112**, 241101 (2014) arXiv:1403.3985.
- [25] M. J. Mortonson and U. Seljak, JCAP **1410**, 035 (2014) arXiv:1405.5857.
- [26] R. Flauger, J. C. Hill and D. N. Spergel, JCAP **1408**, 039 (2014) arXiv:1405.7351.
- [27] C. Cheng, Q. G. Huang and S. Wang, JCAP **1412**, no. 12, 044 (2014) arXiv:1409.7025.
- [28] Q. G. Huang, K. Wang and S. Wang, Phys. Rev. D **93**, no. 10, 103516 (2016) arXiv:1512.07769.
- [29] M. Grana, Phys. Rept. **423**, 91 (2006) [hep-th/0509003].
- [30] M. R. Douglas and S. Kachru, Rev. Mod. Phys. **79**, 733 (2007) [hep-th/0610102].
- [31] F. Denef, M. R. Douglas and S. Kachru, Ann. Rev. Nucl. Part. Sci. **57**, 119 (2007) [hep-th/0701050].
- [32] F. Denef, arXiv:0803.1194.
- [33] L. C. Price, H. V. Peiris, J. Frazer and R. Easther, Phys. Rev. Lett. **114** (2015) no.3, 031301 arXiv:1409.2498.
- [34] A. R. Liddle, A. Mazumdar and F. E. Schunck, Phys. Rev. D **58**, 061301 (1998) [astro-ph/9804177].
- [35] P. Kanti and K. A. Olive, Phys. Rev. D **60**, 043502 (1999) [hep-ph/9903524].
- [36] P. Kanti and K. A. Olive, Phys. Lett. B **464**, 192 (1999) [hep-ph/9906331].
- [37] N. Kaloper and A. R. Liddle, Phys. Rev. D **61**, 123513 (2000) [hep-ph/9910499].
- [38] R. Easther and L. McAllister, JCAP **0605**, 018 (2006) [hep-th/0512102].
- [39] S. Dimopoulos, S. Kachru, J. McGreevy and J. G. Wacker, JCAP **0808**, 003 (2008) [hep-th/0507205].
- [40] S. A. Kim and A. R. Liddle, Phys. Rev. D **74**, 023513 (2006) [astro-ph/0605604].
- [41] S. A. Kim and A. R. Liddle, Phys. Rev. D **76**, 063515 (2007) arXiv:0707.1982.
- [42] F. Vernizzi and D. Wands, JCAP **0605**, 019 (2006) [astro-ph/0603799].
- [43] T. Battefeld and R. Easther, JCAP **0703**, 020 (2007) [astro-ph/0610296].
- [44] R. Easther, J. Frazer, H. V. Peiris and L. C. Price, Phys. Rev. Lett. **112**, 161302 (2014) arXiv:1312.4035.
- [45] Andreas Winkelbauer, arXiv:1209.4340.
- [46] D. V. Hinkley, Biometrika **56**, 635 (1969).